Vapor Flow into a Capillary Propellant-Acquisition Device

F. T. Dodge* and E. B. Bowles†
Southwest Research Institute, San Antonio, Texas

An analytical model is described that specifies the conditions needed to cause a flow of vapor through the screens of a start basket. The analytical model is composed of several original submodels that interrelate the evaporation of the liquid in the basket, the bubble-point change of a screen in the presence of wicking, the drying out of a screen through a combination of evaporation and pressure difference, the vapor flow rate across a wet screen as a function of pressure difference, and the effect on wicking of a difference between the static pressure of the liquid reservoir and the vapor surrounding the screen. Most of the interrelations were verified by a series of separate-effects tests, which were also used to determine certain empirical constants. The equations of the model were solved numerically for typical start-basket designs. A simplified start basket was constructed and tested to verify these predictions, using both volatile and nonvolatile liquids. The test results verified the trends predicted by the model.

Nomenclature

a = empirical friction coefficient in screen flow-through equation (dimensionless)
A_i = interfacial area between main liquid volume and vapor
A_0 = outer surface area of start basket exposed to heat fluxes
A_{vs} = surface area (screen plus liquid) of vapor space
A_{wet} = area of inner main screens wet on both sides
b = screen thickness
b_f = effective thickness of screen open to wicking
C = screen-wicking geometric resistance factor (dimensionless)
D_p = bubble-point diameter
F = screen flow-through geometric factor
F_j = concentrated flow resistance of window-screen/main-screen junction
K_1,K_2,K_3,K_4 = empirical factors, see Eqs. (11), (18), (22), and (24)
l = wetted or wicking length of window screen
$\dot{m}_e$ = internal liquid evaporation rate per unit area
$\dot{m}_0$ = external liquid evaporation rate per unit screen area
$\dot{m}_s$ = flow across main screen from main liquid volume to channel volume per unit screen area
$\dot{m}_w$ = evaporation rate from window screen per unit area
$\dot{M}_v$ = vapor flow across window screen
P = vapor space pressure
P_{cu} = channel liquid pressure at top of basket
P_0 = external vapor pressure
P_{sat} = liquid saturation pressure
R = gas constant of vapor
t = time
T = liquid temperature
V = vapor space volume
ΔP_{0v} = P_0-P
ΔP_{0ms} = P_0-P_{cu}
μ_L,μ_0 = viscosity of liquid and vapor
ρ_L,ρ_0 = liquid and vapor density
$\phi,\bar{\phi}$ = capillary wicking constant with and without an imposed pressure differential across screen

Subscripts

ms,ws = parameter evaluated for the main screen or the window screen, respectively

Submitted March 14, 1983; presented as Paper 83-1380 at the AIAA 19th Joint Propulsion Conference, Seattle, Wash., June 27-29, 1983; revision received July 13, 1983.

*Institute Engineer. Department of Mechanical Sciences. Associate Fellow AIAA.
†Research Engineer, Department of Mechanical Sciences.

Introduction

SPACECRAFT that require a restarting of liquid propellant engines must have some propellant over the engine inlets even after adverse disturbances. A general class of capillary devices called "start baskets" has been used successfully for this purpose in applications where the propellants are storable. For cryogenic propellants, unavoidable heat transfer may, however, cause local boiling which would drive liquid out of the basket or let vapor in. The effectiveness of the baskets might thereby be diminished. As a result, there has been much research aimed at characterizing and understanding capillary acquisition systems for cryogenic propellants.[1-4]

Incorporating a "window" screen in the design has been advanced as one way of overcoming the unfavorable effects of cryogenic propellant boiling. Previously, an extensive experimental program meant to quantify the behavior of such designs was conducted, but the program was only partially successful because of a lack of repeatability in the test data.[1] In particular, it was found that short periods of vapor inflow were followed by longer periods of no inflow when small models of start baskets were tested, but for larger models the inflow was more or less continuous. The reasons for such differences were not apparent. Thus, a number of questions remained about the way the window screen, the main screens, and the vapor and liquid flows interact. The research presented in this paper was designed to answer such questions as well as to develop quantified relations that can be used to design start baskets.

Analysis

The analysis is developed with the aid of the simplified design sketched in Fig. 1. The weave of the window screen is more open than that of the main screens; thus, the bubble-point pressure of the window screen is less. The screens in-

tercept the external heat leak fluxes, with the result that liquid $\dot{m}_0$ is evaporated from the screen surfaces. Capillary action then sets up a liquid withdrawal rate $\dot{m}_s$ from the main liquid volume V_L that keeps the channels formed by the main screens full of liquid. The exterior surfaces of the main screens therefore remain wetted and continue to act as a heat barrier. However, the liquid withdrawal creates a vapor space V in the basket; by proper geometric shaping of the basket, the vapor can be made to stay in contact with the window screen. Eventually, the window screen may dry out partially or the vapor pressure P may become so low in comparison to the exterior pressure P_0 that a gas flow $\dot{M}_v$ is established across the window screen. Note that the inflow always occurs across the window screen because of its smaller bubble-point pressure; hence the name "window screen."

Response of Vapor Space

To simplify the analysis, the vapor is treated as an ideal gas having a molecular weight not too different from the exterior gas. The pressure change in the vapor space is therefore,

$$\frac{dP}{dt} = \frac{P}{V}\left(\frac{dV}{V}\right) + \frac{RT}{V} + (\dot{m}_e A_{vs} + \dot{M}_v) \tag{1}$$

The vapor volume and liquid level variations are given by

$$\frac{dV}{dt} = (\dot{m}_0 A_0 + \dot{m}_e A_{vs})/\rho_L \tag{2}$$

and

$$A_i \frac{dh}{dt} = \frac{dV}{dt} \tag{3}$$

Pressure and Flow in Channel

The low-velocity flow $\dot{m}_s$ which occurs where the internal surfaces of the main screens are wet on both sides, is related to the pressure differential ΔP across the screens by[5,6]:

$$\dot{m}_s(x,z) = \rho_L \Delta P/\mu_L a_{ms} F_{ms} \tag{4}$$

where F_{ms} is a geometric parameter that depends on the screen weave.[5] (The subscript ms denotes the main screen, ws the window screen.) Since the change of ΔP along the channel length is negligible, Eq. (4) can be integrated over the wetted surface to compute the total flow into the chanels, which must be equal to the evaporation rate $\dot{m}_0 A_0 + \dot{m}_e A_{vs}$. The pressure P_{cu} in the channels at the junction with the window screen can therefore be related to the flow rates:

$$P_{cu} = P_0 - (\Delta P_{0v} - \Delta P_{lv}) - \rho_L g h - (\dot{m}_0 A_0 - \dot{m}_e A_{vs}) \times \mu_L a_{ms} F_{ms}/A_{wet} = P_0 - \Delta P_{0ms} \tag{5}$$

Here ΔP_{lv} is the pressure difference between the surface of the main liquid and the vapor volume; for a storable liquid ΔP_{lv} is negligibly small, but for a cryogen or near-boiling liquid $\Delta P_{lv} = P_{sat} - P$. ΔP_{0v} is the difference between the exterior pressure and the vapor space pressure. The parameter ΔP_{0ms} combines, for convenience, all of these effects into one pressure difference.

Wicking Along Window Screen

Any liquid evaporated from the window screen must be replaced by capillary-induced wicking from liquid in the channels. Thus, even though the window screen may remain wet, there is a liquid flow in the plane of the screen. The maximum possible magnitude of the flow depends on the wicking suction pressure P_σ which is a function of both the screen weave and the liquid surface tension. The relation giving this maximum flow is derived most clearly if the screen is imagined to be dry with a front of wicking liquid advancing into it; the liquid is supplied from a reservoir, as depicted for the window screen in Fig. 1. If l is the wetted length at time t and the wicking velocity V_w is dl/dt, the maximum possible wicking velocity is related to the pressures as[7]:

$$P_{cu} - P_\sigma = C_{ws}\mu_L l\left(\frac{dl}{dt}\right)\Big/ b^2 ws \tag{6}$$

where C_{ws} is a nondimensional geometric factor that must be determined experimentally for each screen type. In previous analyses[1,7] it has been tacitly assumed that the wicking reservoir and screen are both exposed to the same environmental pressure (for example, the atmosphere). In that case

$$P_{cu} - P_\sigma = \phi_{ws}\sigma/D_{pws} \tag{7}$$

D_{pws} is the bubble-point diameter of the window screen and ϕ_{ws} is an experimentally determined parameter that relates the wicking "pore" diameter to the bubble-point diameter. Equation (6) then can be integrated to give a wicking length prediction as a function of time that is useful in experimental determinations of C_{ws}:

$$l = \left[2\left(\frac{\phi b^2}{D_p C}\right)_{ws}\left(\frac{\sigma t}{\mu_L}\right)\right]^{1/2} \tag{8}$$

When the screen and the reservoir are at different static pressures, it is not legitimate to use Eq. (7). Instead, P_σ and P_{cu} must be related to the same reference pressure, say, the exterior pressure P_0, and the net wicking suction is then

$$P_\sigma = P_0 - \phi_{ws}\sigma/D_{pws} \tag{9}$$

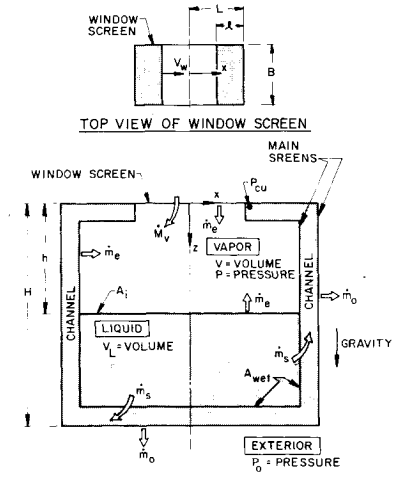

Fig. 1 Nomenclature for analysis of start basket.

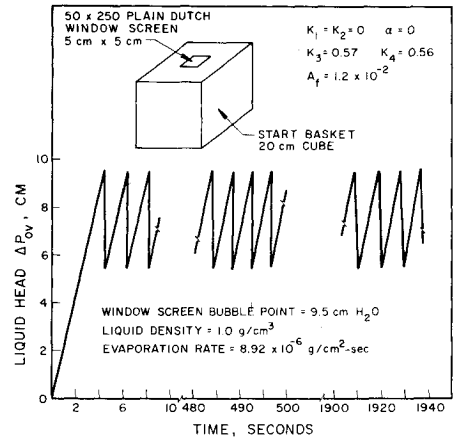

Fig. 2 Typical cyclical inflow.

From Eq. (5), the reservoir is $P_{cu} = P_0 - \Delta P_{0ms}$, so Eq. (6) now should be rewritten as:

$$\frac{\phi_{ws}\sigma}{D_{pws}} - \Delta P_{0ms} = C_{ws}\mu_L l \frac{dl}{dt} \Big/ b_{ws}^2 \tag{10}$$

Note that the decrease of P_{cu} with respect to P_0 diminishes the ability of the screen to remain wet in the presence of evaporation.

When there is also a pressure difference $\Delta P_{0v} = P_0 - P$ across the screen thickness, part of the capillary potential must be used to resist ΔP_{0v} and is not available to create a wicking flow. It is assumed here that P_σ decreases linearly with an increase in ΔP_{0v}:

$$\phi_{ws} = \bar{\phi}_{ws}\left\{1 - K_1\left[\frac{\Delta P_{0v}}{(4\sigma/D_{pws})} - \left(1 - \frac{1}{K_1}\right)\right]\right\} \tag{11a}$$

for $\Delta P_{0v} \geq [1 - (1/K_1)]4\sigma/D_{pws}$, and

$$\phi_{ws} = \bar{\phi}_{ws} \tag{11b}$$

for $\Delta P_{0v} < [1 - (1/K_1)]4\sigma/D_{pws}$. The form of Eqs. (11) will be explained later in conjunction with Eq. (18). Note that $\phi_{ws} = 0$ when $\Delta P_{ov} = 4\sigma/D_{pws}$ and, that there is no decrease of the wicking when ΔP_{0v} is nonzero but small. K_1 is a non-dimensionnal geometric screen parameter that must be determined experimentally; $\bar{\phi}_{ws}$ is the value of ϕ_{ws} when $\Delta P_{0v} = 0$ and is a property of the screen weave; and $4\sigma/D_{pws}$ is the bubble-point pressure.

The actual wicking velocity in the screen is

$$\frac{dV_w}{dx} = \frac{\dot{m}_w}{\rho_L b_{fws}} \tag{12}$$

where b_{fws} is an effective "open" thickness of the screen. [That is, Bb_{fws} is the cross-sectional area of the screen open to a wicking flow. Conceptually, b_{fws} can be related to b_{ws}, the true screen thickness, by imagining it to be the width of a flow channel. Then, Eq. (6) could be written for laminar flow as

$$P_{cu} - P_\sigma - 12\mu_L l\left(\frac{dl}{dt}\right) \Big/ b_{fws}^2 \tag{13}$$

which gives, by comparison

$$b_{fws} = b_{ws}/(C_{ws}/12)^{1/2} \tag{14}$$

For accuracy, b_{fws} should be determined experimentally as described later.]

By manipulating the differential form of Eq. (1) in conjunction with Eq. (12) and the appropriate boundary conditions, the liquid pressure at a point x in the wicking film can be shown to be

$$P_w(x) = P_0 - \Delta P_{0ms} - \frac{\mu_L l^2 \dot{m}_w}{2\rho_L b_{ws}^2 b_{fws}} \times \left\{C_{ws}\left[1 - \left(\frac{x}{l} - \frac{L}{l} - 1\right)^2\right] - \frac{2F_j b_{ws}^2}{l}\right\} \tag{15}$$

The maximum wetted length l of the window screen in the presence of evaporation can be found from Eq. (15) by setting $x = L - l$ (see Fig. 1) and $P_w = P_0 - \phi_{ws}\sigma/D_{pws}$. It is the solution of

$$l^2 + 2l\left(\frac{F_j b_{ws}^2}{C_{ws}}\right) - \frac{2\rho_L b_{ws}^2 b_{fws}}{\mu_L \dot{m}_w C_{ws}}\left(\frac{\phi_{ws}\sigma}{D_{pws}} - \Delta P_{0ms}\right) = 0 \tag{16}$$

If $l > L$, the screen remains completely wet; otherwise, an area $2B(L-l)$ will dry out. The maximum possible evaporation rate that still lets the window screen remain wet can be found from Eq. (16) by setting $l = L$.

$$(\dot{m}_w)_{max} = \frac{2b_{ws}^2 b_{fws}}{L^2 C_{ws}}\left(\frac{\rho L \bar{\phi}_{ws}\sigma}{\mu_L D_{pws}}\right) \tag{17}$$

(The system parameters F_j and ΔP_{0ms} have been neglected here in order to derive a relation involving only liquid and screen-weave properties.)

Bubble Point of Window Screen

Since the interfacial curvatures of the liquid at the screen surfaces are affected by the wicking (i.e., part of the available capillary potential is used to drive the wicking), the bubble point of the screen should decrease when a wicking flow exists; it is assumed here that the decrease is linearly related to the wicking flow.

$$(\Delta P_{0v})_{max} = \frac{4\sigma}{D_{pws}}\left\{1 - K_2\left[\frac{\Delta P_w}{(\bar{\phi}\sigma/D_p)_{ws}}\right]\right\} \tag{18}$$

K_2 is an experimentally determined geometric parameter defined here, and ΔP_w is the wicking pressure drop along the screen. Since ΔP_w is related to the actual evaporation from the screen and $\bar{\phi}_{ws}\sigma/D_{pws}$ is related similarly to the maximum possible wicking (evaporation) rate, Eq. (18) can be written alternately as:

$$(\Delta P_{0v})_{max} = \frac{4\sigma}{D_{pws}}\left[1 - K_2 \dot{m}_w/(\dot{m}_w)_{max}\right] \tag{19}$$

By inserting Eq. (17) into Eq. (19), the bubble-point decrease also can be expressed in terms of $\dot{m}_w$ and screen and liquid parameters:

$$(\Delta P_{0v})_{max} = \frac{4\sigma}{D_{pws}}\left[1 - K_2\left(\frac{\dot{m}_w \mu_L D_{pws} L^2 C_{ws}}{2\rho_L \bar{\phi}_{ws}\sigma b_{ws}^2 b_{fws}}\right)\right] \tag{20}$$

A somewhat analogous effect of evaporation on bubble point has been reported elsewhere,[8] where it was found that the bubble point slowly decreased as liquid evaporated from a wet screen. This was an unsteady phenomenon, as contrasted to Eq. (20), but a similar behavior might occur in start baskets during ground testing, as will be discussed later.

Because of the reciprocal nature of the phenomena modeled by Eqs. (11) and (18), it is evident that K_1 is simply $1/K_2$, i.e., $d\phi_{ws}/d\Delta P_{0v} = 1/(d\Delta P_{0v}/d\phi_{ws})$. Further, if the screen is wet, the bubble point must be greater than zero. Thus, the total possible range of ΔP_{0v} must be the same for both Eqs. (11) and (18), and algebraic manipulation shows that the form given for Eqs. (11) is the only one consistent with Eq. (18).

Previous tests have shown that after the bubble-point pressure of a screen has been exceeded, the pressure differential must be reduced in order to make the screen reseal.[9] Thus, the pressure-drop resistance of the screen is assumed here to be

$$\Delta P_{0V} = P_0 - P \geq (\Delta P_{0v})_{max} \tag{21}$$

to initiate an inflow, after which

$$\Delta P_{0v} \leq K_3 (\Delta P_{0V})_{max} \tag{22}$$

to cause resealing. From test data[9] it appears that $K_3 \approx 0.57$.

Flow Through the Window Screen

When the central area of the window screen dries out or ΔP_{0V} exceeds the bubble point, vapor will flow into the basket. If the screen dries out, the inflow can be computed by Eq. (4) with the gas properties used rather than liquid:

$$\dot{M}_v = 2\rho_0 \Delta P_{0v}(L - l)B/\mu_0 a_{ws} F_{ws} \tag{23}$$

Table 1 Wicking flow characteristics

Screen	Thickness, b, $\times 10^{-4}$ cm	Bubble-point diameter, D_p, $\times 10^{-4}$ cm	Wicking direction relative to warp wire	C	$\bar{\phi}$	$b(12/C)^{1/2}$, $\times 10^{-4}$ cm	b_f, $\times 10^{-4}$ cm
50×250	368	105	Perpendicular	338	0.393	69	143
			Parallel	584	0.231	52	Not determined
24×110	940	275	Perpendicular	507	0.428	144	118
			Parallel	1369	0.533	88	Not determined
165×800	147	40	Perpendicular	476	1.128	23	Not determined
			Parallel	1548	1.047	13	Not determined
200×1400	135	19	Perpendicular	1962	0.225	10.6	Not determined
			Parallel	1525	0.318	12.0	Not determined

When the bubble point is exceeded, however, a "dry" area cannot be identified, and Eq. (23) is not valid. It has been proposed that this type of inflow should be based upon the difference between ΔP_{0V} and the bubble-point pressure.[1] Taking into account also the need to allow for "re-sealing" and the observation from the present tests that vapor flows through only a small fraction of the wetted area, the proposed method of computing the inflow is:

$$\dot{M}_v = 2\rho_0 [\Delta P_{0v} - K_4 (\Delta P_{0v})_{\max}] A_f LB/\mu_0 a_{ws} F_{ws} \quad (24)$$

Here A_f is an empirical constant that determines the fraction of the wet screen penetrated by the flow. The empirical factor K_4 must not be greater than the resealing fraction K_3 or else an outflow can be predicted.

Evaporation Rates

The evaporation rate from the external surfaces of the main and window screens will normally be driven by heat transfer, but the internal evaporation rate, $\dot{m}_e$, is not, since the main channels "intercept" all of the external heat. For near-boiTherefore, it is proposed to compute the internal evaporation rate by

$$\dot{m}_e = \alpha (P_{sat} - P)/\sqrt{RT}, \qquad P < P_{sat} \quad (25a)$$

$$\dot{m}_e = 0, \qquad P \geq P_{sat} \quad (25b)$$

Typically the empirical constant α ranges from about 10^{-4} to 1. The temperatures of the main liquid must decrease to supply the required heat of vaporization. Solving such a complicated heat-transfer problem is outside the scope of the present work; instead, the liquid temperature is assumed to remain constant. This assumption can be used only to study trends, because, in fact, the liquid will stratify with the colder liquid (and lower P_{sat}) near the surface.

Solution of Equations

A Runge-Kutta integration routine was used to solve the preceding set of equations for many typical cases. Some of the important findings include the following.

1) After ΔP_{0v} first exceeds the bubble-point pressure, the screen subsequently almost always is predicted to dry out because $\phi_{ws}\sigma/D_{pws} - \Delta P_{0ms}$ becomes negative and Eq. (10) predicts a dewicking flow. ΔP_{0v} then changes to a new value such that $\phi_{ws}\sigma/D_{pws} - \Delta P_{0ms} = 0$, which halts the dewicking. The amount of dry area adjusts itself so that the inflow is just sufficient to maintain this ΔP_{0v}. The screen does not reseal. It is unlikely that this is the real behavior of a window screen, because the channel suction ΔP_{0ms} will not rupture the liquid layer in the window screen and cause an actual drying out. Instead, it would just pull liquid back into the channels by decreasing the liquid layer thickness, and the screen would remain wet. (The thinning of the liquid layer decreases the bubble-point pressure, and the response of the window screen might be erratic in tests.)

In order to study the other parameters, dewicking due to ΔP_{0ms} was suppressed in the calculations described in the following cases.

2) The response of the window screen is sensitive to the rate of internal evaporation. In fact, it can be seen from Eqs. (1), (3), and (25) that inflow can be prevented when α is large enough:

$$\alpha \geq P_{sat} A_i \left(\frac{dh}{dt}\right) / (A_{vs} \Delta P_{0v} \sqrt{RT})$$

Since $\sqrt{RT}$ is a large number, the computed values of α are within the reasonable range of 10^{-4} to 1.0.

3) Cycling of the inflow (alternating periods of window-screen breakdown and resealing) cannot occur either when the window screen dries out from evaporation or when $K_4 = K_3$.

4) If $K_4 < K_3$, cycling of the inflow is possible. The pressure difference $\Delta P_{0v} - K_4 (\Delta P_{0v})_{\max}$ remains greater than zero, with the result that after an initial sharp drop of the vapor space pressure, the inflow rate is larger than that needed to balance dV/dt and the vapor space pressure begins to increase. At some point ΔP_{0v} increases to $K_3 (\Delta P_{0v})_{\max}$ and the screen reseals. The process then repeats itself. Figure 2 shows some results for a typical case 4. The cycling frequency initially is short but increases as the vapor space volume increases. (For these computations, K_4 has been taken as 0.56, K_3 as 0.57, and A_f as 1.2×10^{-2}.)

Experimental Program, Results, and Discussion

The experimental program had two main objectives: 1) to validate the various submodels and determine the empirical constants contained in them, and 2) to verify the predictions of the entire model for a simulated start basket. The first objective was met by a series of separate-effects tests. To achieve the second objective a simplified start basket was built and tested. Two different liquids—isopentane with a 28°C boiling point, and ethanol with a 118°C boiling point—were used to study the relative effects of evaporation. The test screens were washed, cleansed, and dried using the procedures described elsewhere,[7] and the tests were conducted under controlled temperature and humidity conditions, generally in the presence of an atmosphere saturated with the vapor of the test liquid.

Separate-Effects Tests

Experimental determinations were made of:

1) Wicking resistance coefficient, C.
2) Wicking pressure constant, $\bar{\phi}$.
3) Bubble-point diameter, D_p.
4) Effective open thickness, b_f.
5) Decrease of bubble-point pressure due to wicking, K_2.
6) Flow resistance of window-screen/main-screen joint, F_j.
7) Degradation of window-screen bubble-point, due to the joining method.

Items 4 and 5 were measured only for the window-screen candidates (50×250 and 24×110 plain dutch) since they are not needed in the analysis of the main screens (165×800 and 200×1400 twilled dutch). Data on $C/\bar{\phi}$ and D_p are available in the literature for some screen types; that data served as checks on the results of this study.

Wicking Characteristics

C and $\bar{\phi}$ were determined with the apparatus shown schematically in Fig. 3. The test screen could be oriented horizontally or vertically. In the horizontal configuration the reservoir was filled until the liquid almost touched the screen at the knife edge. To start the test, liquid was rapidly added to the reservoir until the liquid surface was level with the knife edge; liquid would then wick along the screen. The reservoir was maintained level with the knife edge during the entire test. The leading edge of the wicking liquid was measured as a function of time with a graduated scale attached to the clamps. Each test was continued until the wicking velocity became small or evaporation became important. Test procedures for the vertical configuration were similar.

Figure 4 shows typical results of the measured horizontal wicking distance l plotted against the square root of wicking time. As shown by Eq. (8), the slopes of the resulting straight lines are related to the wicking parameters, and $C/\bar{\phi}$ can therefore be determined from such plots. The vertical wicking tests were used to determine the parameter $\bar{\phi}$; since the maximum wicking distance, $H_{\max}$, measured during vertical tests is the hydrostatic head that just balances the wicking suction pressure, $\bar{\phi}$ is given by $\bar{\phi}=\rho_L g H_{\max} D_p/\sigma$. Values of C and $\bar{\phi}$ computed from the test data are given in Table 1. The wicking constant $\bar{\phi}$ is about one-tenth to one-fourth of the bubble-point parameter (i.e., 4), depending on the screen weave and wicking direction. The wicking resistance C tends to increase for the more closely woven screens, as might be expected.

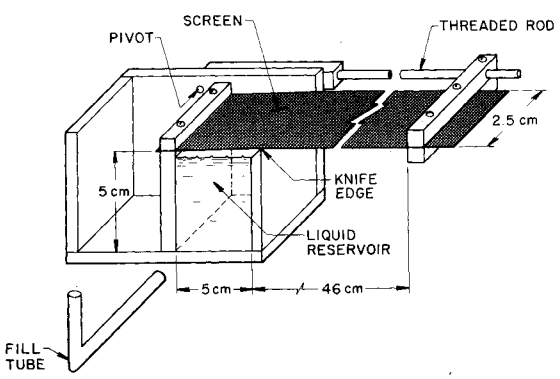

Fig. 3 Cutaway view of "screen and joint characterization" apparatus.

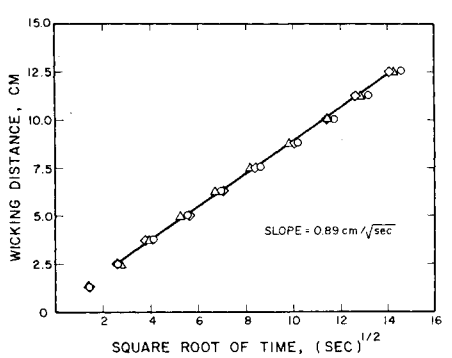

Fig. 4 Ethanol wicking perpendicular to warp wires of 24×110 plain dutch screen.

Joint Flow Resistance

To determine F_j of typical junctions, samples of the 50×250 and 165×800 screens and the 24×110 and 200×1400 screens were joined by electrical-resistance spot welding and tested in the apparatus shown in Fig. 3. The tests showed that the flow resistance of a well-manufactured joint was negligible.

Bubble Point

The bubble points for all of the test screens were measured in order to have a common basis for determining any change in bubble point caused by evaporation. Figure 5 shows the apparatus used for these tests. The test screen was inserted into the apparatus and clamped to make a leakproof seal. Ethanol or isopentane was then poured on the screen to form a pool 0.6 cm deep. The pressure in the chamber below the screen, which was measured by a water manometer, was then increased slowly. The pressure at which gas bubbles were observed to penetrate the liquid was taken as the bubble point (after correcting for the 0.6 cm head). It was noted that the chamber pressure had to be reduced in order to make the screens reseal, in agreement with Ref. 9. The computed bubble-point diameters, as shown in Table 1, are the same as or slightly smaller (that is, the bubble-point pressures are larger) than other results.[3]

Combinations of window and main screens were also tested. Even though each spot-welded joint could be made tight enough that the bubble point was equal to that of the window screen alone, the bubbles always broke through the seam first.

Next a series of tests was conducted to determine K_2. Several different evaporation rates had to be established in

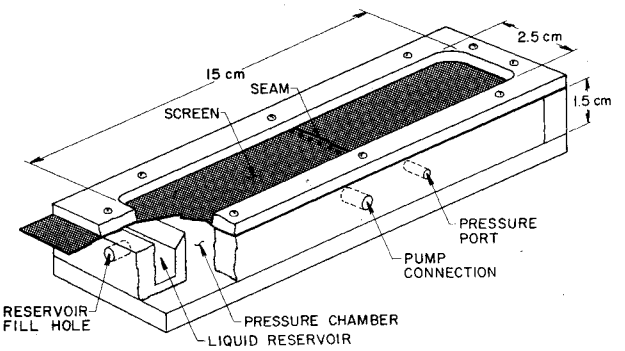

Fig. 5 Cutaway view of bubble-point evaporation" apparatus.

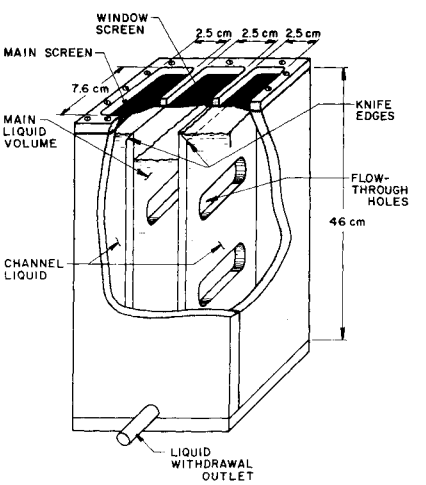

Fig. 6 Cutaway view of simplified start basket.

order to vary the wicking velocity. Because of difficulty in maintaining repeatable evaporation rates with ethanol, only the lower boiling-point isopentane was used. The evaporation rate was regulated by first placing the entire apparatus in an ice bath and then letting it slowly heat to room temperature. A series of bubble-point tests with increasing rates of evaporation thereby could be conducted. The test measurements are presented in Table 2. $(\dot{m}_w)_{\max}$ are the rates for which it appeared that any further increase in evaporation would not have allowed the screens to remain completely wet. [Since $\dot{m}_w$ could not be adjusted arbitrarily, there is some judgment involved as to what was $(\dot{m}_w)_{\max}$.] For both screens the measurements indicate that $K_2 = 0.5$ (and thus $K_1 = 2.0$). Data for the two main screens and for the window screens in their less effective wicking direction were not acquired since these K_1 and K_2 are not needed in applications.

The effective open thickness, b_f, of the window screens was computed from the $(\dot{m}_w)_{\max}$ data by the use of Eq. (17) with $l = L = 7.62$ cm, the length of the test screen. The computed values are shown in Table 1, as well as the values of $b(12/C)^{1/2}$ derived from a capillary channel analogy. The channel analogy yields values that are not markedly different from the measured ones and thus could be used to estimate b_f in the absence of other data.

Start Basket Tests

Figure 6 shows a schematic of the start basket used in the tests. It consisted primarily of a window screen attached to a pair of main screens and a clear plastic "basket." Evaporation was simulated by draining liquid from the main volume. The channel and main liquid volumes communicated through a series of holes drilled in the walls; the effective depth of the start basket was controlled by blocking all the holes above any specified height. The window and main screens were held in place over knife edges by rubber gaskets that were compressed by a set of upper and lower plastic clamps. Proof tests showed that the resulting seal was leak-tight for vacuum pressures equal to at least the largest expected bubble-point of the main screens. Wicking from the main screens to the window screens did not appear to be affected by the clamping force at the knife edges. The pressure in the liquid volume was measured with an accuracy of 0.3 cm of liquid by an electronic pressure transducer connected to a digital voltmeter. The liquid level was read directly from graduated scales attached to the walls. At the start of a test all three volumes were full of liquid and contained no visible bubbles. For tests using isopentane, the entire apparatus was cooled for several hours in a freezer before conducting tests in order to control the evaporation rate.

Tests were conducted initially using window screens joined to the main screens by spot welds, with the joints near and parallel to the knife edges. These tests gave repeatable data, but in every case gas first broke through at the weld seam, even though the measured ΔP_{0v} was equal to the expected bubble-point pressure. ΔP_{0v} then slowly decreased to about 20% of the bubble point, where it appeared to stabilize. During some of the tests, the draining was halted to verify that the vapor space vacuum could be maintained, thus proving that the window screen did act as a seal. The gravity head h (Fig. 1) eventually exceeded the bubble point of the main screens; gas then flowed through all of the screens.

The ΔP_{0v} response was not anticipated in the light of previous tests where a cyclic inflow was obtained[1] or from bubble-point testing where the screens were found to reseal after ΔP fell below about 57% of the bubble point.[9] (At this time, the real significance of the decreased pressure ΔP_{0ms} in the channel volumes had not yet been appreciated.) The tests were therefore repeated, using a double-screen arrangement that eliminated all weld seams. (A main screen was fabricated to cover the entrances to all three channels. The central area of this screen was cut out to uncover the main volume just inside the knife edges. A window screen, also large enough to cover all three channel entrances, was laid over the main screen and bolted down with the upper clamp. The bubble point of the main volume thus remained equal to that of the window screen, while the bubble point of the channels remained equal to that of the main screens. Preliminary testing showed that wicking from the channel liquid to the window screen was not impeded.) The test results were not markedly different than before. Figures 7 and 8 show measurements from two typical tests and the computed values of $\Delta P_{0ms} = \Delta P_{0v} + h$. The window screen appeared to break down initially as a result of ΔP_{0v} exceeding the bubble point, rather than by drying out as a result of evaporation. The effect of evaporation from the window screen is apparent in the isopentane results, however, since the initial bubble point

Table 2 Decrease of maximum pressure differential as a function of evaporation rate; wicking perpendicular to warp wire

Screen	Evaporation rate, g/s-cm^2	Bubble point, cm of H_2O	Maximum ΔP, cm of H_2O
50×250	6.61×10^{-5}	6.1	6.1
	7.54×10^{-5}	6.1	5.33
	3.37×10^{-4} $(\dot{m}_w)_{\max}$	6.1	3.05
24×110	7.08×10^{-5}	2.5	2.5
	8.78×10^{-5}	2.5	2.50
	1.52×10^{-4}	2.5	2.30
	2.16×10^{-4}	2.5	2.03
	4.65×10^{-4} $(\dot{m}_w)_{\max}$	2.5	1.25

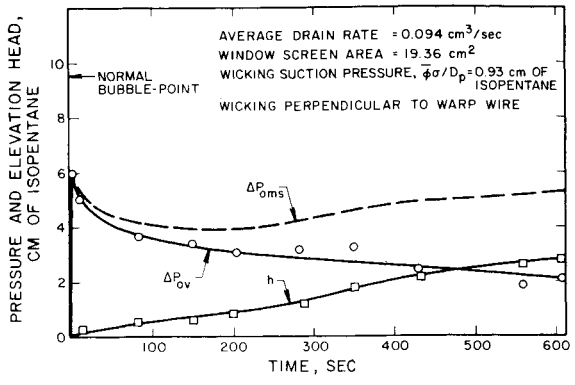

Fig. 7 Response of start basket containing isopentane.

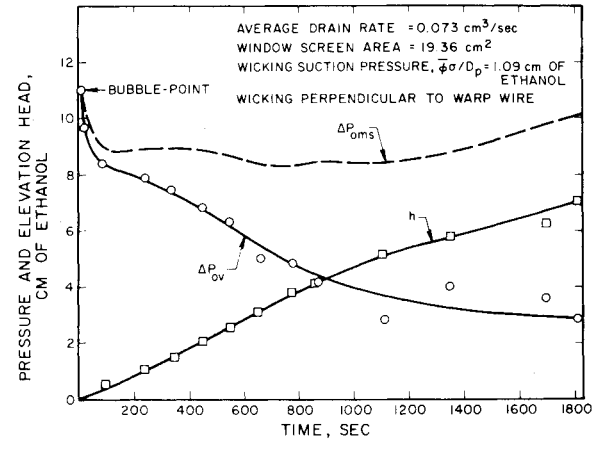

Fig. 8 Response of start basket containing ethanol.

was only 63% of normal. For both ethanol and isopentane, ΔP_{0v} gradually decreased to about 25% of the bubble point. Occasionally, the liquid outflow would be halted during the time when ΔP_{0v} had stabilized. It was found that ΔP_{0v} would decrease by about 0.5 – 1.0 cm of liquid, a change that apparently represents the pressure difference required to maintain the inflow across the wet screen. Using tabulated properties[13] of the screen to compute F_{ws}, Eq. (24) was used to show that the value of A_f is on the order of 10^{-2}.

It was concluded that the continuous decrease of ΔP_{0v}, and the absence of cyclic inflow, was a result of ΔP_{0ms} exceeding the capillary suction, $\phi\sigma/D_p$, of the window screen. That would lead to a gradual thinning of the liquid layer in the window screen. The effect is the same as evaporation from a screen that is not in contact with a supply of wicking fluid; the bubble point gradually decreases in such cases.[9] To verify this conclusion, several tests were conducted in which small amounts of liquid were periodically added directly to the window screen in order to replenish any liquid withdrawn into the channels. (The amounts were sufficient only to wet the screen, and did not form a pool.) ΔP_{0v} was found to increase immediately after adding the liquid, which indicates therefore that the liquid layer on the screen had been thinned.

The start-basket tests reported by others[1] are also understandable in terms of a thinning of the liquid layer in the window screen. In one configuration, the window screen had a very small surface area and communicated directly with a large reservoir by an arrangement that formed a small pool of liquid in the space between the window screen and the main screen. Cycling of the inflow was observed. Evidently, the small window screen and its attachment method allowed edge effects to keep the window screen completely wet for a time. The liquid suction head in the channel liquid eventually became large enough, however, to cause the window screen to dry out. Then the response was similar to that shown in Fig. 7 or 8. When larger window screens were tested, cycling inflow was not observed consistently. The thickness of the liquid layer in the window screen probably decreased rapidly as a result of the channel liquid vacuum, ΔP_{0ms}, analogously to the tests of this study.

The overall behavior of the simulated start basket, although initially unexpected, is concluded to be in agreement with the predictions of the analytical models developed in this study.

Conclusions and Recommendations

Several new models have been developed that predict:

1) Decrease in the bubble point pressure of a screen in the presence of wicking.

2) Decrease of the wicking ability of a screen in the presence of a pressure differential across the screeen thickness.

3) Effective open area of a screen for wicking flow.

4) Conditions for the drying out or the vapor penetration of a screen that is simultaneously wicking and resisting a pressure difference.

5) Vapor inflow rate as a function of pressure difference across a *wet* screen.

6) Effect on wicking of a difference between the environmental pressure of the liquid reservoir and screen.

All of these relations were needed to assess the performance of a start basket, and more parameters were needed to characterize the screen than just D_p and $C_w/\bar{\phi}$, the parameters usually measured and for which data were available. Separate-effects tests were conducted to verify models (1 – 4) above and to determine the empirical constants appearing in them. It was concluded that the models are successful in quantitatively predicting the correct functional dependence of the important parameters.

The equations of the entire model were solved for typical start-basket designs. The computed results show that: 1) evaporation of liquid into the vapor can control the response of the start basket by maintaining an internal pressure sufficient to prevent the breakdown of the window screen; 2) cycling of the inflow may occur when the heat load is not sufficient to dry out the window screen; and 3) the liquid pressure in the channels decreases as the pressure in the vapor space decreases, and at some point the resultant vacuum pressure in the channels may exceed the wicking suction pressure of the window screen, after which the liquid layer in the screen will thin and the bubble point will decrease. When case 3 occurs, the ΔP across the window screen can decrease to levels below that which would normally cause the window screen to reseal. Whether the inflow then cycles is dependent upon the design of the start basket and the gravity level.

A simplified start basket was constructed and tested to verify the predictions. The results did verify the trends predicted by the model, but quantitative comparisons could not be made because the data needed to evaluate the constants in models 5 and 6 above were not available and could not be determined from the test results.

For that reason, further separate-effects tests are recommended:

1) The relation between the gas flow rate across a wet screen, the imposed pressure difference, and the screen bubble point should be quantified.

2) The postulated effect of decreasing the liquid reservoir pressure on the ability of a screen to wick should be verified.

3) The rate of liquid layer thinning, and its effect on the bubble point, as a function of reservoir pressure should be determined also.

With the results of the recommended tests, the analytical model of vapor inflow into start baskets can be quantified for all conditions of interest.

Acknowledgments

This work was sponsored by NASA Lewis Research Center under Contract NAS3-22664. The advice of the NASA Program Manager, E.P. Symmons, is gratefully acknowledged.

References

[1] Blatt, M. H. and Risberg, J. A., "Study of Liquid and Vapor Flow into a Centaur Capillary Device," General Dynamics/Convair, San Diego, Calif., GDC-NAS-79-001; also, NASA CR-159657, 1979.

[2] Blatt, M. H. and Walter, M. D., "Centaur Propellant Acquisition System Study," General Dynamics/Convair, San Diego, Calif., CASD-NAS-75-023; also, NASA CR-134811, 1979.

[3] Cady, E. C., "Effect of Transient Liquid Flow on Retention Characteristics of Screen Acquisition Systems," McDonnell Douglas Astronautics, Huntington Beach, Calif., MDC G6742; also, NASA CR-135218, 1977.

[4] Bingham, P. E. and Tegart, J. R., "Wicking in Fine Mesh Screens," AIAA Paper 77-849, July 1977.

[5] Armour, J. C. and Cannon, J. N., "Fluid Flow Through Woven Screens," *AIChE Journal*, Vol. 14, May 1968, pp. 415-420.

[6] Bernardi, R. T., Lineham, J. H., and Hamilton, L. H., "Low Reynolds Number Loss Coefficients for Fine-Mesh Sreens," *Transactions of ASME Journal of Fluids Engineering*, Vol. 98, Dec. 1976, pp. 762-763.

[7] Symons, E. P., "Wicking of Liquids in Screens," NASA TN D-7657, May 1974.

[8] Simon, E. D., "Environmental Requirements for Bubble Pressure Tests on Fine-Mesh Screens," *Journal of Spacecraft and Rockets*, Vol. 16, July-Aug. 1979, pp. 218-222.

[9] Paynter, H. L., "Acquisition/Expulsion System for Earth Orbital Propulsion System, Volume III, Cryogenic Test," Martin Marietta Corp., Denver, Colo., MCR-73-97, 1973.

[10] Hirth, J. P. and Pound, G. M., *Condensation and Evaporation Growth Kinetics*, Macmillan Co., New York, 1963.

[11] *Chemical Engineers' Handbook*, edited by J. H. Perry, 4th Ed. McGraw-Hill Book Co., New York, 1963, pp. 4-48.

[12] Boublik, T., Fried, V., and Hala, E., *The Vapour Pressure of Pure Substances*, Elsevier Scientific Publishing Co., 1973.

[13] "Low Gravity Propellant Control Using Capillary Devices in Large Scale Cryogenic Vehicles. Design Handbook," General Dynamics/Convair, San Diego, Calif., GDC-DDB70-066, 1970.